# Magnetic Pulse Welding of the “Tube – Plug” Pair of STS410 Steel*

**V. Krutikov[1], S. Paranin[1], V. Ivanov[1], A. Spirin[1], D. Koleukh[1], J.-G. Lee[2], M.-K. Lee[2], C.-K. Rhee[2]**

[1] Institute of Electrophysics of the Ural Branch of Russian Academy of Sciences (IEP), Russian Federation
[2] Korea Atomic Energy Research Institute (KAERI), Republic of Korea

## Abstract

*The research was focused on the magnetic pulse welding (MPW) of 12.5% Cr steel STS410. The experiments were performed in the tube-plug geometry (both details were made of the same steel). Magnetic pulse unit consisted of pulsed current generator (PCG) loaded to a single-turn coil. Magnetic field amplitude of 40 T was generated in the coil during experiments. The amplitude of pulsed current reached 750 kA.*

*The effects of energy storage capacity, charging voltage, and end plug shape were studied. The welded samples were investigated by optical microscopy. The optimal velocities of impact and contact front motion were evaluated as 300 m/s and 3-3.5 km/s, respectively.*

*The paper includes the leakage test results as well. To date, the joints with a helium leak rate of $10^{-9}$ mbar·l·s$^{-1}$ have been produced.*

## Keywords

Welding, Steel, Magnetic Pulse Welding

---

* This work is based on the results of the Joint Research Project between KAERI in Korea and IEP in Russia (Agreement № 13/13) supported by KAERI R&D Program. This work is also supported by Russian Foundation for Basic Research (project № 13-08-00883-a) and Ural Branch of the Russian Academy of Sciences (project № 12-Y-2-1029).

# 1 Introduction

The widely used steel STS410 (identical in chemical composition to AISI 410) is employed for a variety of applications due to its high heat- and corrosion-resistance. However, the welding process is still an issue. The development of approaches, which facilitate the production of high quality joints, is very important.

A candidate method of making joints is magnetic pulse welding [1,2] (MPW) due to the following reasons:

- MPW has proven repeatability and high processing rate.
- The obtained joint has high mechanical strength and large area [3].
- The produced joint does not adversely affect the heat treatment and microstructure of the steels, so the procedure does not require preliminary and post-weld heat treatment.

The purpose of this study was to find a range of optimal parameters for MPW in geometry of tube - end plug in terms of the largest welding area and the best weld seam microstructure.

# 2 Experiment

The tubes and end plugs were machined from an extruded bar. The sample's surface was not treated after the manufacturing process. Table 1 presents the chemical composition of STS410.

| C, % | Si, % | Mn, % | P, % | S, % | Cr, % | Fe, % |
|---|---|---|---|---|---|---|
| 0.15 | 1.00 | 1.00 | 0.040 | 0.030 | 12.50 | Bal. |

***Table 1:*** *Chemical composition of STS410*

The magnetic pulsed unit consisted of pulsed current generator (PCG) loaded to a single-turn coil (inductor). The generator was based on the capacitors battery that consisted of 36 capacitors connected in parallel. The battery was discharged to inductor by 12 triggered vacuum switches (1 switch per 3 capacitors module). The total PCG capacity, C, was 425 μF, the charging voltage, $U_0$, was up to 25 kV. A half of the battery was used in several experiments (in that case the capacity was 210 μF). The current oscillation period was 27 and 20 μs at capacities of 425 and 210 μF, respectively (Figure 1a). The single-turn inductor, made of hardened steel, had the working diameter of 8.8 mm and the length of 12 mm.

For the experiments reported here typical PCG parameters were the following: charging voltage was 8.5 kV; magnetic field amplitude in empty coil was 37 T and peak current was 700 kA.

The typical geometry of the welding parts was the same as in [3,4]. The thin-wall steel tube was welded to inner steel end plug. Figure 1b shows a schematic diagram of the experimental setup. Under magnetic pressure copper driver together with steel tube were accelerated radially inward and collapsed to the end plug. Copper was used as a driver material due to its high electric conductivity and low mechanical strength. Collapse velocity is one of the critical parameters in the welding process. The tapered shape of the end plug (Figure 2a) helps to achieve the impact front motion along the plug surface. The contact front velocity is the second critical parameter of the welding process. Certain values of the impact and contact front velocities are required to make a good weld seam [2], and different materials or material's combinations have their own values.

The parameters of magnetic pulse, tube strength and initial acceleration gap between tube wall and end plug surface determined the impact velocity. In turn, the contact front velocity was determined by impact velocity and the end plug taper angle.

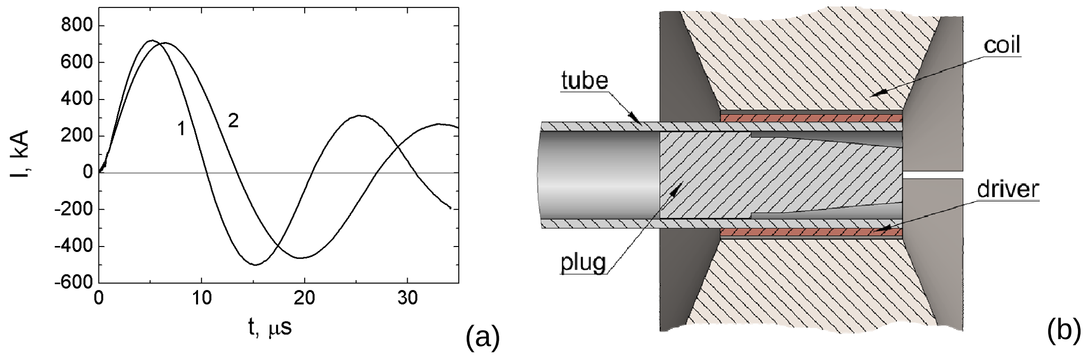


***Figure 1:** a – typical current wave-forms at different circuit parameters (C[µF]/$U_0$[kV]): 1 – 210/13, 2 – 425/8.5; b – schematic diagram of MPW experiment*

The steel tubes of 7 mm in outer diameter and of 0.6 mm in thick were used. The copper driver of 8 mm in outer diameter and 0.5 mm in thick slipped over the end of the tube prior to welding without any inserted insulator between the driver and the tube.

The intensive plastic deformation of near-contact volumes during high velocity impact leads to the solid-state bonding of the tube to the plug [2,5].

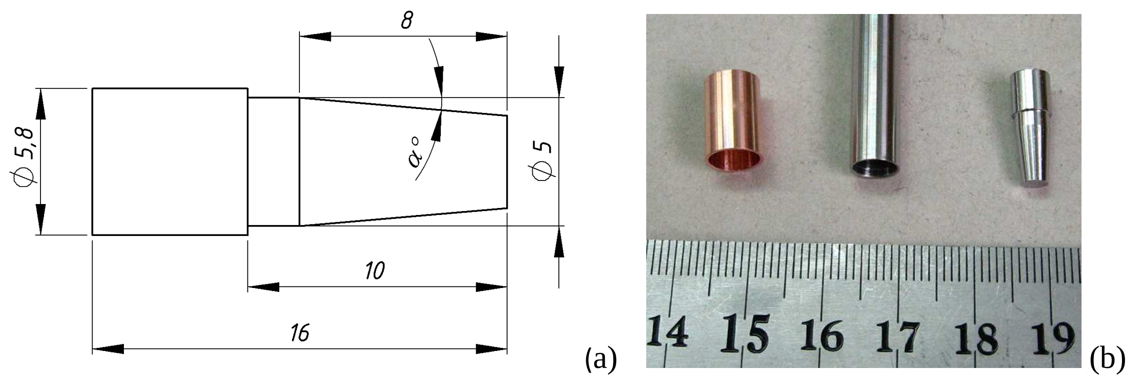


***Figure 2**: a – end plug design; b – welding parts view*

The longitudinal sections of the welded samples were made in order to investigate weld seam properties. The samples were cut in the plane that coincides with the inductor slit. So, the photomicrography shows two weld segments: one of those close to the coil slit and the other one on the opposite side.

The obtained sections were investigated with optical metallographic microscope Olympus BX-41RF.

The leakage tests were carried out with helium leak tester.

For microstructure investigations the sample surfaces were chemical etched with hydrochloric acid and ethanol in proportion of 1:1 at room temperature [6].

# 3 Results and Discussion

## 3.1 Weldability Window

The PCG charging voltage, battery capacity and plug taper angle α (Figure 2a) were varied during the experiments.

The different sample's photomicrographs of longitudinal sections were superposed into bigger pictures (see Figure 3). The weld seam on these pictures looked like a confluence between tube and plug materials. The discernible boundary (black line) between the tube and end plug is an absence of joint. The lengths of the weld seams and diameters on the plug cone at weld starting point were measured on these pictures.

Typical experiment results are described in Table 2. The charging voltage, battery capacity, and end plug taper angle were varied. First, the charging voltage at which welding starts was defined. For the full PCG capacity of 425 μF it was 8 kV. For a half of the capacity (210 μF) it was about 12 kV. The comparison of the weld seam lengths (Table 2) demonstrated that for the full capacity the optimal parameters were: 8.5 kV charging voltage and 5° taper angle. For 9.5 kV cha rging voltage the narrow end of the plug was destructed (Figure 3c).

For a half of the generator capacity (Samples C25, C26) the current half-period T/2 decreased from 13.6 μs to 10.0 μs. In case of 13 kV charging voltage, the current amplitude was 720 kA. That current amplitude could be reached if the generator with the full capacity had charged to 8.7 kV.

| # | α, [°] | $U_0$, [kV] | C, [μF] | $I_m$, [kA] | T/2, [μs] | $L_1$, [mm] | $L_2$, [mm] | $d_1$, [mm] | $d_2$, [mm] |
|---|---|---|---|---|---|---|---|---|---|
| C18 | 5 | 7,0 | 425 | 592 | 13,5 | no weld | | | |
| C21 | 5 | 8,0 | 425 | 670 | 13,4 | 6,69 | 2,92 | 4,74 | 4,47 |
| C23 | 5 | 8,5 | 425 | 704 | 13,4 | 6,57 | 6,96 | 4,71 | 4,83 |
| C24 | 5 | 8,5 | 425 | 704 | 13,4 | 7,12 | 5,20 | 4,58 | 4,61 |
| C28 | 5 | 8,5 | 425 | 708 | 13,5 | 6,22 | 4,81 | 4,58 | 4,67 |
| C27 | 3 | 8,5 | 425 | 704 | 13,6 | 2,56 | 6,11 | 4,32 | 4,69 |
| C19 | 5 | 9,0 | 425 | 748 | 13,8 | 6,94 | 7,15 | 4,67 | 4,80 |
| C22 | 5 | 9,5 | 425 | 808 | 13,4 | 3,92 | 5,15 | 4,67 | 4,80 |
| C25 | 5 | 11,0 | 210 | 604 | 10,0 | no weld | | | |
| C26 | 5 | 13,0 | 210 | 720 | 10,0 | 7,21 | 7,41 | 4,79 | 4,85 |

***Table 2:*** *MPW experiments data*

*Table notes: C – battery capacity; $U_0$ – charging voltage, $I_m$ – current amplitude, T/2 – current half-period, $L_1$, $L_2$ – weld seam lengths, $d_1$, $d_2$ – diameters on the plug cone at weld starting point. Subscripts 1 and 2 correspond to the weld seams at the opposite side and close to the inductor slit.*

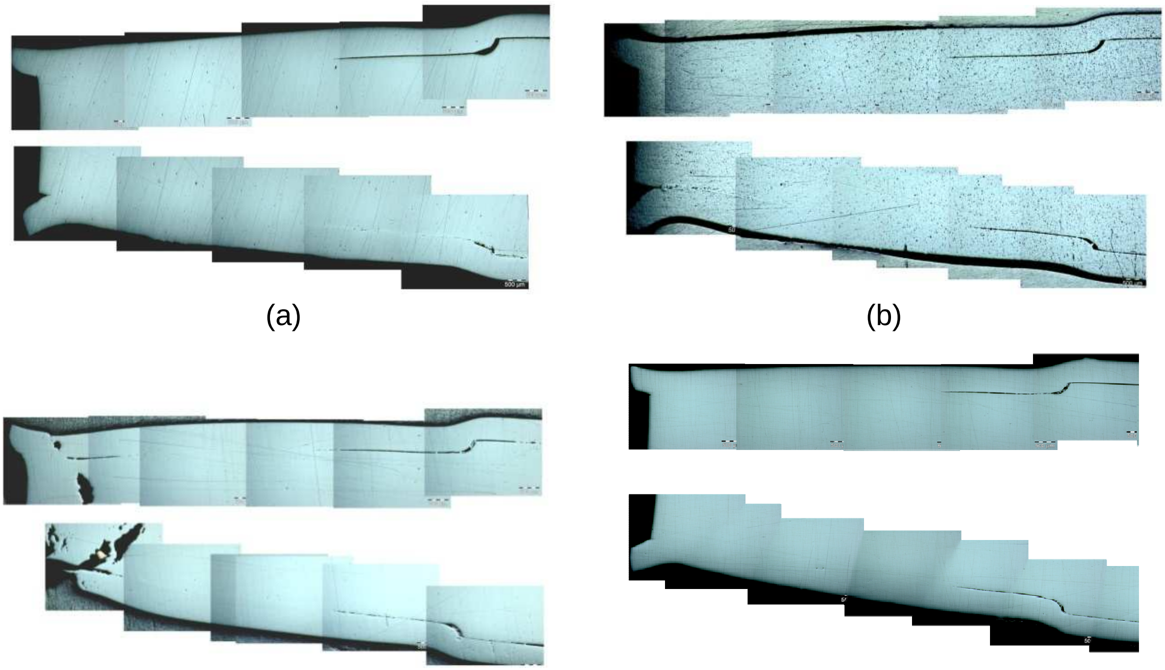

(a) (b)

(c) (d)

***Figure 3:*** *Optical microscopy of the polished surfaces (longitudinal section) of the samples obtained at different MPW conditions (C[µF]/U$_0$[kV]): a – 425/8.5 (Sam. #C23), b – 425/9.0 (#C19), c – 425/9.5 (#C22), d – 210/13.0 (#C26)*

## 3.2 Welding conditions estimation: collapse velocity and contact front speed

For the inductor in the absence of the welding sample, the ratio of the generated magnetic field to the discharge current, $B_m/I_m$, was measured to be 0.053 T/kA. At MPW experiments the amplitude of magnetic field was estimated using this ratio. It should be noted that this estimation gives slightly lower value of $B_m$. Typical values of the estimated magnetic field amplitude were about 40 T.

Table 3 summarizes the calculated parameters of magnetic pulse welding process.

They are the velocities of impact $V_i$ and the contact front motion $V_{ki}$ at the time moments, $t_i$, when the welding started. The subscripts *1* and *2* refer to the parameters which were calculated for the certain joint segments position with respect to the inductor slit, namely, *1* – opposite position, *2* – close to the inductor slit. Generally, these parameters differed due to the magnetic field nonuniformity close to the inductor slit.

The time moment $t_i$, when the inner tube diameter became equal to $d_i$ (see Table 2), and the velocity $V_i$ at this moment were estimated by the solution of the equation describing radial motion in a compressing copper–steel tube. The velocity ($V_{ki}$) of contact point motion was determined as

$$V_{ki} = V_i / \sin \alpha \quad (1).$$

The comparison of $t_i$ values shows that, for $C$ = 425 µF, welding starts prior to attaining a maximum value of magnetic field and approximately in maximum at $C$ =

210 µF, $U_0$ = 13 kV. It should be emphasized that the last parameters gave the best quality of weld. Under optimal conditions, $V_i$ values are about 300 m/s while $V_{ki}$ values are about 3-3.5 km/s.

As shown in [2], a joint is usually failed if the joint speed $V_k$ exceeds a sound speed in material. Therefore, the results, obtained for the samples with the angle of 3°, are well consistent with literature data. In this case, the joint speed of 6.9 km/s was higher than the sound speed in the steel (6.25 km/s for STS410).

| # | α, [°] | $I_m$, [kA] | $B_m$, [T] | $t_1$, [µs] | $V_1$, [m/s] | $V_{k1}$, [km/s] | $t_2$, [µs] | $V_2$, [m/s] | $V_{k2}$, [km/s] |
|---|---|---|---|---|---|---|---|---|---|
| C19 | 5 | 748 | 40 | 5.9 | 300 | 3.4 | 5.7 | 270 | 3.1 |
| C21 | 5 | 670 | 36 | 6.3 | 260 | 3.0 | 6.6 | 300 | 3.5 |
| C22 | 5 | 808 | 43 | 5.7 | 310 | 3.7 | 5.5 | 290 | 3.4 |
| C23 | 5 | 704 | 37 | 6.0 | 270 | 3.2 | 5.8 | 250 | 3.0 |
| C24 | 5 | 704 | 37 | 6.2 | 295 | 3.6 | 6.1 | 290 | 3.5 |
| C28 | 5 | 708 | 38 | 6.2 | 300 | 3.5 | 6.1 | 280 | 3.3 |
| C27 | 3 | 704 | 37 | 6.6 | 340 | 6.9 | 6.1 | 280 | 5.7 |
| C26 | 5 | 720 | 38 | 5.0 | 290 | 3.4 | 4.9 | 280 | 3.3 |

***Table 3:*** *The calculated parameters of MPW process*

*Table notes: $B_m$ – magnetic field amplitude; $t_1$, $t_2$ – time when welding starts; $V_1$, $V_2$ – tube wall impact velocities at welding start.*

## 3.3 Leakage testing

The samples, successfully welded at the C[µF]/$U_0$[kV]: (1) 425/8.5 and (2) 210/13, were tested on the helium leakage. For the first sample group the leak rate was less than $2.0 \times 10^{-9}$ mbar·l·s$^{-1}$. For the next sample group the leak rate as low as $1.0 \times 10^{-9}$ mbar·l·s$^{-1}$ was achieved. Obtained results confirm high quality of welding, according to the results reported in [3,4].

## 3.4 Weld seam and bulk microstructure

Figure 4 shows the etched surface micrographs of the specimens joined at different conditions of magnetic pulse welding. In all cases, we observed smaller size material grains in the vicinity of the weld seam: the effect became more pronounced with increasing $U_0$. The best results were obtained at $U_0$ = 8.5 kV. The seam exhibited a characteristic wavy structure and the area of complete interpenetration. The joint thickness did not exceed 2 µm.

Thus, the comparison of the samples weld zone microstructure showed that the best weld was achieved at 8.5 kV among the samples welded at 425 µF. In this mode, the amplitude of the discharge current was 700 kA, and the corresponding amplitude of the magnetic field was at a level of 37-40 T.

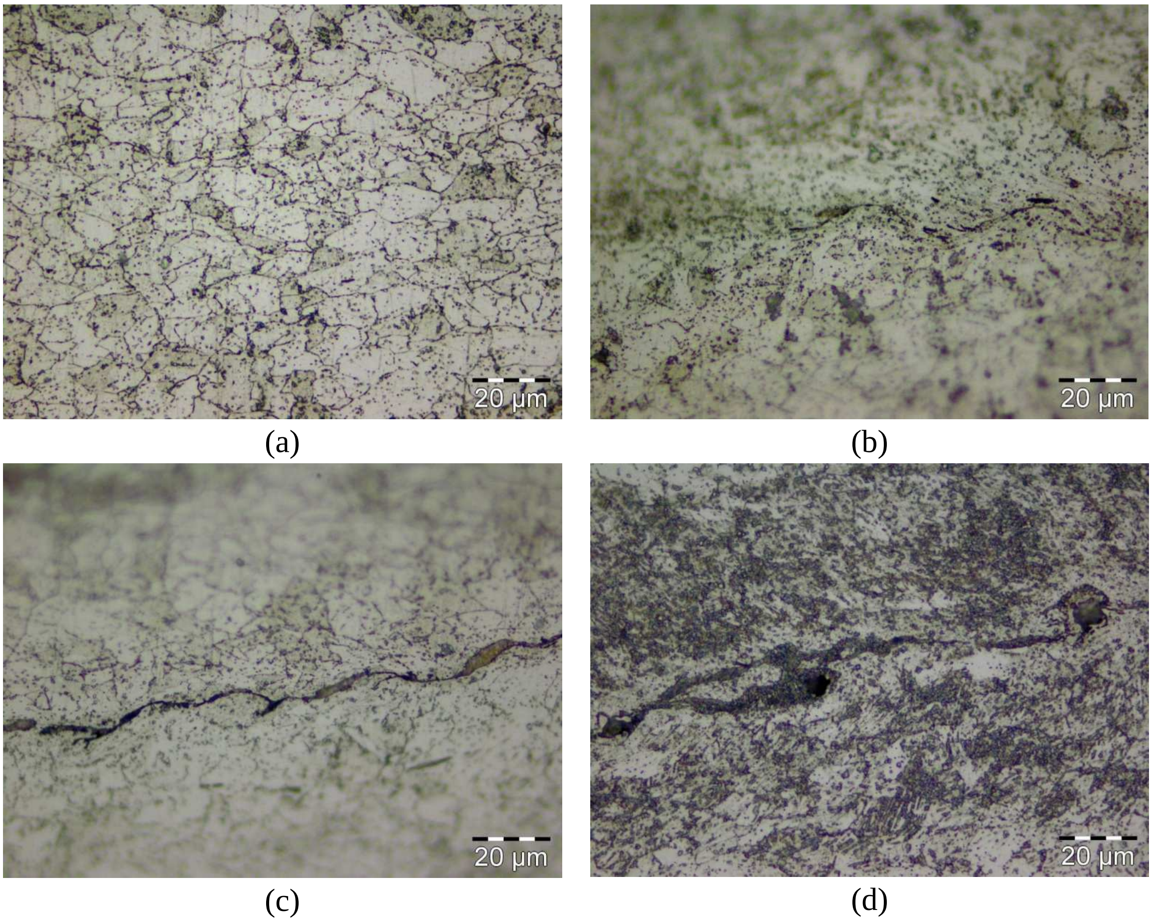


***Figure 4:*** *Optical microscopy of the polished and etched surfaces (longitudinal section): bulk region – a; weld seam at* $U_0$*=8.5 kV – b,* $U_0$*=8.0 kV – c,* $U_0$*=9.5 kV – d (capacity – 425 µF)*

## 4 Conclusions

The magnetic pulse welding of the steel STS410 has been investigated. The experiments were performed in the geometry of “tube – plug”. The optimum welding conditions were found. The most appropriate impact velocity was about 300 m/s at the contact point velocity of 3-3.5 km/s. For achieving the required magnetic field amplitude (40 T at the period length of 20-27 µs), the current amplitude of 700-750 kA was employed at the inductor with the working length of 12 mm.

The leakage test showed a good helium tightness at the level of $1\times10^{-9}$ mbar·l·s$^{-1}$.

The weld microstructure in comparison of different samples confirmed that the optimum value of current amplitude was 700 kA. The weld was wavy and with several areas where both metals were completely fused. The grain refinement was observed near the weld as well.

## References

[1] US Patent № 3126937, Forming method and apparatus therefor. D.F. Brower et. al., 1964

[2] A.A. Dudin. Magnitno-impulsnaya svarka metallov (Magnetic Pulsed Welding of Metals). Moscow: Metallurgiya, 1979, 128 s. – in Russian.

[3] W.F. Brown, J. Bandas, N.T. Olson. Pulsed magnetic welding of breeder reactor fuel pin end closures. Welding Journal, June 1978, p. 22-26.

[4] John McGinley. Electromagnetic pulsed technology as a means of joining generation IV cladding materials. Proceedings of the 17th International Conference on Nuclear Engineering (ICONE17) July 12-16, 2009, Brussels, Belgium

[5] E.S. Karakozov. Soyedinenie metallov v tvyordoj faze (Joining of metals in solid phase). Moscow: Metallurgiya, 1976. – 264 s – in Russian.

[6] M. Bekkert, H. Klemm. Spravochnik po metallographicheskomu travlenijy. (Metallographic etching hand-book). Moscow: Metallurgiya, 1979. – 336 s. – in Russian.